SESSION 4. DYNAMICS AND OPTIMIZATION

Session Chairman

R. J. Melosh*

Philco-Ford Corp.
Palo Alto, California

*now with Virginia Polytechnic Institute and State University, Blacksburg, Va.

The Transient Dynamic Analysis of Thin Shells by the Finite Element Method*

Samuel W. Key
Zelma E. Beisinger
Sandia Laboratories
Albuquerque, New Mexico 87115

A simple central difference time integration scheme along with a diagonal mass matrix is used to examine the transient dynamic response of linear elastic thin shells. The numerical stability of the explicit time integration scheme is examined and two inequalities are provided, the strongest of which defines a critical time step. Only calculations using a time step less than the critical time step are meaningful. Above the critical time step, the calculations diverge. The method is called conditionally stable. One inequality is based on membrane behavior and the other on bending behavior. Both of them are in terms of minimum mesh dimensions, shell densities and membrane and bending moduli. The diagonal mass matrix is generated from a consistent mass matrix in a rational manner. Three calculations are included to show the results of this work.

*This work was supported by the United States Atomic Energy Commission.

The Transient Dynamic Analysis of Thin Shells by the Finite Element Method

1. INTRODUCTION

In many respects, the transient dynamic linear analysis of thin shells is well in hand. There is a need, however, for continued improvement in computational speed while maintaining the accuracy of the results, particularly with two dimensional meshes being introduced and larger and larger problems being considered. Two methods are available to obtain improved computational times. A diagonal mass matrix can be used in place of the consistent or non-diagonal matrix prescribed by the finite element method, [1,2], and explicit time integration schemes in place of the implicit schemes can be used.

In the finite element literature, there is no clear cut preference for any one form of mass matrix nor any one method of integration. Although, the unconditionally stable implicit time integration schemes have won many adherents.

Wilson and Clough[3] adopted an implicit linear acceleration scheme, one of the Newmark β methods. It is a conditionally stable scheme. Clough and Felippa[4] in examining plate vibration problems conclude that lumped mass matrices are as accurate or more accurate than the non-diagonal mass matrices prescribed by the finite element method. In their lumped mass calculations, only the translational inertias are retained with the rotations eliminated by static condensation. Clough[5] in a survey of their work reiterates their use of the linear acceleration integration scheme. The paper contains a clear statement of their preference of the lumped mass matrix in place of the consistent mass matrix. Clough and Wilson[6] refer to a new linear acceleration scheme to integrate in time. It is the previous scheme coupled with a predictor-corrector scheme for the accelerations. The result is an unconditionally stable method.

Klein and Sylvester[7] adopt the unconditionally stable implicit time integration scheme of Chan, Cox and Benfield[8] along with the non-diagonal mass matrix of the finite element method.

Stricklin, et al.,[9] selected the unconditionally stable implicit time integration scheme of Houbolt[10], using a non-diagonal mass matrix for transient calculations. For the calculation of mode shapes and frequencies, they use a diagonal mass matrix, retaining the rotational degrees of freedom in the deflections normal to the shell,[11]. Their procedure

for generating the diagonal mass matrix is the same as the one adopted below but they provide no rationale for the choice of the scale factor introduced.

Fu[12] advocates the use of the de Vogelaere[13] method for integrating in time. The method is again an unconditionally stable implicit scheme.

Olson and Lindberg[14] in examining the vibration behavior of curved plates use a consistent mass matrix. Part of their results are obtained neglecting inplane inertia. Whether these degrees of freedom are eliminated by static condensation or simply set to zero to give a bending only response is unclear. The study is impressive.

Greene, Jones and Strome[15] in examining the vibrational modes of cylindrical panels consider both consistent and lumped mass matrices. In both cases, various freedoms are retained with the others being eliminated by static condensation. The result is a preference for the diagonal mass matrix. In none of their lumped mass calculations were rotational degrees of freedom retained.

One of the more informative pieces of work in the finite element literature on numerical time integration is a paper by Nickel[16], the result of an earlier entanglement with an unconditionally unstable implicit scheme.

Goudreau[17] has an extensive treatment of the behavior of various mass matrices in membrane and bending behavior along with an examination of several methods of integration in time. A diagonal mass matrix and a conditionally stable implicit time integration scheme are preferred. It is remarked

that the higher frequencies are inaccurate in the discrete equations and should be suppressed in any event. The remark is based on frequency error versus wave length plots for exact time integration. Key and Krieg[18] have re-examined this question in the light of discrete time integration and show that the higher modes may have quite accurate frequencies and should not necessarily be suppressed.

In explicit time integration schemes, the mass matrix M times the vector of accelerations $\ddot{q}$ occurs, $M\ddot{q}$. In order to find the accelerations which are used to advance the velocities and the displacements, this set of equations must be solved. If M is a diagonal mass matrix, then the solution is trivial. In the finite difference literature, the majority of applications treat only diagonal mass matrices. Implicit integration schemes involve the inverse of a weighted sum of the mass and stiffness matrices, $(b_1M + b_2K)^{-1}$, to find the accelerations. The coefficients b_1 and b_2 depend on the particular implicit scheme being used. If only the non-diagonal mass matrix prescribed by the finite element method is considered, no particular computational advantage is evidenced by either scheme because M^{-1} in the explicit schemes and $(b_1M + b_2K)^{-1}$ in the implicit schemes represent the same amount of computational effort. Thus, the use of a diagonal mass matrix must precede any claim of computational efficiency for the explicit time integration schemes. In the work that follows, a rational approach to generating a diagonal mass matrix from the non-diagonal matrix of the finite element method is discussed.

The major stumbling block to explicit time integration schemes is their conditional stability. Computationally, they are very fast but must use a time step below a certain critical value. If a value above the critical time step is used, then harmonic solutions are represented as exponentially growing solutions and the results are erroneous. Below the critical time step harmonic motion is represented as harmonic motion. The critical time step is invariably related to the shortest transit time between any two nodal points that exist in the finite element mesh. This corresponds to the highest frequency that the system will represent. For impulse problems and suddenly applied temperature and pressure, these frequencies are needed in the solution. Even when implicit schemes are used for these problems, they are used with time steps related to this same criteria just to keep these frequencies present and accurately represent them. They invariably give the same answers as explicit schemes for these problems but at a much greater computational expense. It should be noted that when only the lower modes of response are significant, then unconditionally stable implicit schemes can track them with a large time step while a conditionally stable explicit scheme must remain with what now looks to be a very small time step in relation to the response. However, if a modal solution is used, the explicit schemes again become competitive.

By examining stability, very good estimates of the critical time step are possible. Once this has been done, the explicit

schemes become very reliable and for the problems involving the high frequency response of the shell, they are equally as accurate as the implicit schemes and much faster computationally per time step. The work below considers a simple centered second order difference approximation to the accelerations and provides the critical time step expressions needed to make the computations.

2. STIFFNESS MATRIX

The finite element used for this analysis is a doubly curved arbitrary quadrilateral designed for shells where the reference surface is a portion of an axisymmetric surface. It is based on a minimum potential energy principle and a discrete Kirchhoff hypothesis. There are nine degrees of freedom at each mesh point; the circumferential, meridional and normal displacements along with their first derivatives in the surface variables are carried at each mesh point. The element is pictured in Figure 1. The details of its derivation are well documented in References [19,20,21].

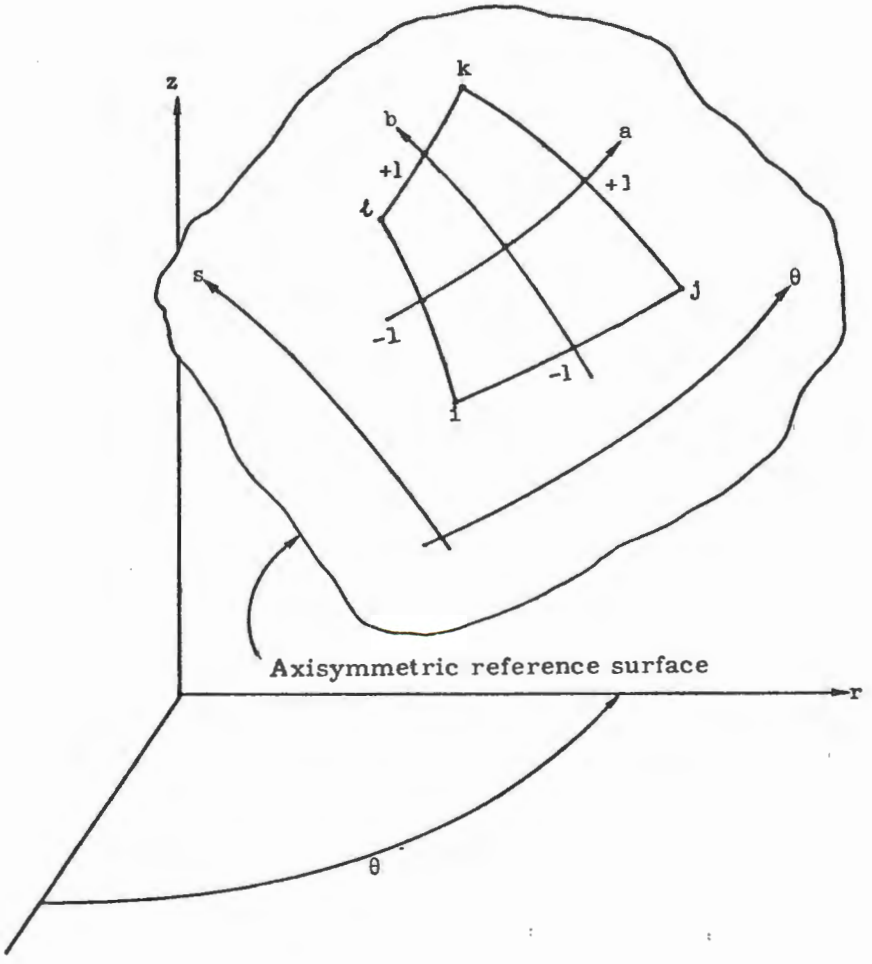

Figure 1. Element Geometry

3. MASS MATRIX

A diagonal or "lumped" mass matrix is used. The approach taken in obtaining it is based on results obtained in simple one dimensional membrane and bending problems which exist as special cases of the more general shell element introduced above.

By taking a cylindrical shell with a very large radius to thickness ratio and zero Poisson's ratio and striking it end on, the same results are obtained as if one were examining the one dimensional wave equation shown in Equation (2).

$$c_m^2 u_{xx} - u_{tt} = 0 \tag{2}$$

Here, u is the axial or meridional displacement of the cylinder, and x and t denote differentiation in space and time respectively. The sound speed c_m is given by the square root of the modulus E divided by the density ρ, $c_m = (E/\rho)^{\frac{1}{2}}$. The thickness of the shell cancels out. For the homogeneous problem considered with homogeneous boundary conditions, Hamilton's principle can be written as shown in Equation (3).

$$\delta \int_{t_1}^{t_2} \int_{x_1}^{x_2} \tfrac{1}{2}\left[(u_t)^2 - (c_m u_x)^2\right] dx dt = 0 \tag{3}$$

In this special case, the original polynomial assumptions contained in the finite element become a cubic in the space variable x. Using the Hermite interpolation form of the cubic polynomial and using an element extending from x_i to x_j, the displacement assumptions can be written as

$$u = u_i h_1(\eta) + u_j h_2(\eta) + u_{x_i} h_3(\eta)\left(\frac{x_j - x_i}{2}\right) + u_{x_j} h_4(\eta)\left(\frac{x_j - x_i}{2}\right) \quad (4)$$

where
$$h_1(\eta) = \tfrac{1}{4}(\eta^3 - 3\eta + 2)$$
$$h_2(\eta) = -\tfrac{1}{4}(\eta^3 - 3\eta - 2)$$
$$h_3(\eta) = \tfrac{1}{4}(\eta^3 - \eta^2 - \eta + 1)$$
$$h_4(\eta) = \tfrac{1}{4}(\eta^3 + \eta^2 - \eta - 1) \quad (5)$$

The local coordinate η runs from -1 to +1. The functions h_1, h_2, h_3, and h_4 are shown in Figure 2.

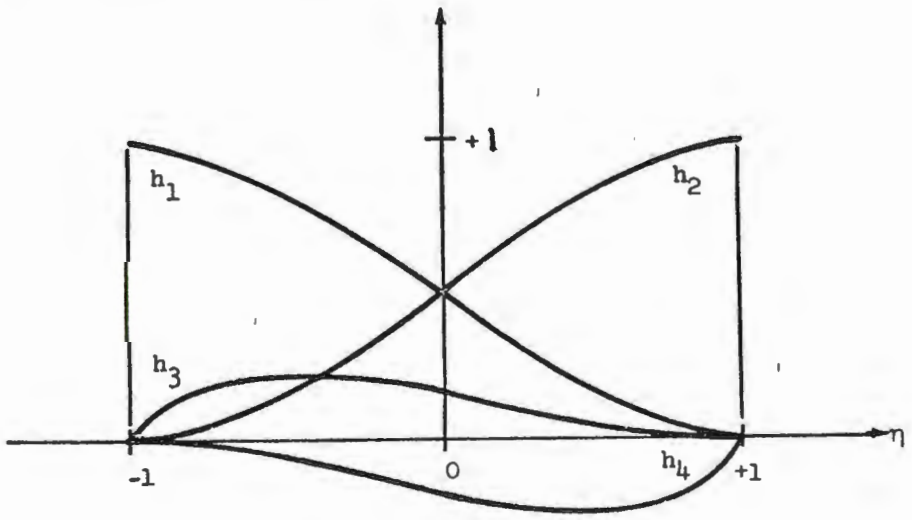

Figure 2. Interpolation functions h_1, h_2, h_3, h_4.

For convenience, the length of the element is written as ℓ in what follows.

The resulting element stiffness is given by Equation (6).

$$k_m = \begin{array}{c} \begin{matrix} u_i & u_{x_i} & u_j & u_{x_j} \end{matrix} \\ \left[\begin{array}{c|c|c|c} \frac{18}{15\ell} & \frac{1}{10} & -\frac{18}{15\ell} & \frac{1}{10} \\ \hline \frac{1}{10} & \frac{4\ell}{30} & -\frac{1}{10} & -\frac{\ell}{30} \\ \hline -\frac{18}{15\ell} & -\frac{1}{10} & \frac{18}{15\ell} & -\frac{1}{10} \\ \hline \frac{1}{10} & -\frac{\ell}{30} & -\frac{1}{10} & \frac{4\ell}{30} \end{array}\right] \end{array} \qquad (6)$$

The resulting element mass matrix is given by Equation (7).

$$m = \begin{array}{c} \begin{matrix} u_i & u_{x_i} & u_j & u_{x_j} \end{matrix} \\ \left[\begin{array}{c|c|c|c} \frac{13\ell}{35} & \frac{11\ell^2}{210} & \frac{9\ell}{70} & \frac{-13\ell^2}{420} \\ \hline \frac{11\ell^2}{210} & \frac{\ell^3}{105} & \frac{13\ell^2}{420} & \frac{-\ell^3}{140} \\ \hline \frac{9\ell}{70} & \frac{13\ell^2}{420} & \frac{13\ell}{35} & \frac{-11\ell^2}{210} \\ \hline \frac{-13\ell^2}{420} & \frac{-\ell^3}{140} & \frac{-11\ell^2}{210} & \frac{\ell^3}{105} \end{array}\right] \end{array} \qquad (7)$$

These are well-known results, and are easily obtained by standard methods in the finite element literature [22,23,24].

Combining the elements into a complete statement of the problem gives Hamilton's principle in the form of Equation (8).

$$\delta \int_{t_1}^{t_2} \tfrac{1}{2}\left[\dot{q}^T M \dot{q} - c_m^2\, q^T K_m q\right] dt = 0 \qquad (8)$$

Here, q is a vector of nodal displacements and displacement gradients and $\dot{q}$ is a vector of nodal velocities and velocity gradients. Lagrange's equations provide the equations of motion(9)

$$M\ddot{q} + c_m^2 K_m q = 0 \qquad (9)$$

The same cylinder subjected to a purely radial load will behave as if one were examining the lateral motion of a uniform beam as shown in Equation (10).

$$c_b^2\, w_{xxxx} + w_{tt} = 0 \qquad (10)$$

Here w is the radial or normal displacement of the cylindrical shell; x and t are again differentiations in space and time, respectively. The constant c_b is given by the square root of the modulus E times the thickness h squared, all divided by 12 times the density ρ, $c_b = (Eh^2/12\rho)^{\frac{1}{2}}$.

For the homogeneous problem considered with homogeneous boundary conditions, Hamilton's principle can be written as shown in Equation (11).

$$\delta \int_{t_1}^{t_2} \int_{x_1}^{x_2} \tfrac{1}{2}\left[\left(w_t\right)^2 - \left(c_b w_{xx}\right)^2\right] dxdt = 0 \qquad (11)$$

Note that rotatory kinetic energy is omitted; it is given by the Expression (12).

$$\int_{t_1}^{t_2} \int_{x_1}^{x_2} \tfrac{1}{2}\left[\frac{h^3}{12}\left(W_{xt}\right)^2\right] dxdt \qquad (12)$$

For bending, the original polynomial assumptions contained in the finite element become a cubic in the space variable x.

Just as before, this is given by Equation (13) for each element.

$$w = w_i h_1(\eta) + w_j h_2(\eta) + w_{x_i} h_3(\eta)\left(\frac{x_j - x_i}{2}\right) + w_{x_j} h_4(\eta)\left(\frac{x_j - x_i}{2}\right) \qquad (13)$$

The resulting element stiffness matrix is given by Equation (14).

$$k_b = \begin{array}{c} \begin{matrix} w_i & w_{x_i} & w_j & w_{x_j} \end{matrix} \\ \left[\begin{array}{c|c|c|c} \frac{12}{\ell^3} & +\frac{6}{\ell^2} & -\frac{12}{\ell^3} & +\frac{6}{\ell^2} \\ \hline +\frac{6}{\ell^2} & \frac{4}{\ell} & -\frac{6}{\ell^2} & \frac{2}{\ell} \\ \hline -\frac{12}{\ell^3} & -\frac{6}{\ell^2} & \frac{12}{\ell^3} & -\frac{6}{\ell^2} \\ \hline \frac{+6}{\ell^2} & \frac{2}{\ell} & \frac{-6}{\ell^2} & \frac{4}{\ell} \end{array}\right] \end{array} \qquad (14)$$

This is a well-known result and easily obtained by standard methods in the finite element literature [22,23,24]. Without rotatory energy terms, the element mass matrix is the same as in the membrane case given by Equation (7).

Combining the elements into a complete statement of the problem gives Hamilton's principle in the form of Equation (15)

$$\delta \int_{t_1}^{t_2} \tfrac{1}{2} \left[\dot{q}^T M \dot{q} - c_b^2 \, q^T K_b q \right] dt = 0 \tag{15}$$

The resulting equations of motion are given by the Expression (16).

$$M\ddot{q} + c_b^2 K_b q = 0 \tag{16}$$

The mass matrices indicated in Equations (9) and (16) are the ones prescribed by the finite element method. They are symmetric and banded and have the same non-zero populations as the stiffness matrices K_m and K_b. Explicit time integration schemes developed in the finite difference literature depend on their ease of application on diagonal or lumped mass matrices, so that M^{-1} is trivial. In order to take advantage of these schemes, it is desirable to replace M with an equivalent diagonal mass matrix M_d. There is of course a considerable amount of literature in the finite difference method on how to create diagonal mass matrices directly and a small amount of work in the finite element literature as well, some of which was covered above.

Consider first only the nodal displacements and their respective mass terms as shown in Equation (17).

$$m = \begin{bmatrix} \frac{13\ell}{35} & \cdot & \frac{9\ell}{70} & \cdot \\ \cdot & \cdot & \cdot & \cdot \\ \frac{9\ell}{70} & \cdot & \frac{13\ell}{35} & \cdot \\ \cdot & \cdot & \cdot & \cdot \end{bmatrix} \tag{17}$$

If the off-diagonal terms are added to the diagonal terms, then the result is shown in Equation (18).

$$m_{11} + m_{13} = \left(\frac{13}{35} + \frac{9}{70}\right)\ell = \frac{\ell}{2}$$

$$m_{31} + m_{33} = \left(\frac{9}{70} + \frac{13}{35}\right)\ell = \frac{\ell}{2} \tag{18}$$

This is not unexpected if rigid body translational kinetic energy is going to be correct for either form of mass matrix. Following this lead, the gradient terms are added to obtain the diagonal inertias shown in Equation (19).

$$m_{22} + m_{24} = \left(\frac{1}{105} - \frac{1}{140}\right)\ell^3 = \frac{\ell^3}{420}$$

$$m_{24} + m_{44} = \left(\frac{1}{105} - \frac{1}{140}\right)\ell^3 = \frac{\ell^3}{420} \qquad (19)$$

As it will turn out, the important aspect of this exercise is that these terms should scale as ℓ^3 rather than ℓ. A diagonal mass matrix is constructed as shown in Equation (20)

$$m_d = \begin{bmatrix} \frac{\ell}{2} & & & \\ & \frac{\alpha\ell^3}{420} & & \\ & & \frac{\ell}{2} & \\ & & & \frac{\alpha\ell^3}{420} \end{bmatrix} \qquad (20)$$

Here, the gradient masses have been multiplied by a parameter α. The bending problem has rigid body rotations as well as the rigid body translations. However, if α is used to give the correct rotational kinetic energy for a single element rotating about its center of gravity, then a negative α will result giving negative gradient inertias. The membrane problem has no other rigid body motions but translation.

It remains to select α. The maximum frequencies of the membrane and bending problems serve as a guide for this selection.

A study of the maximum eigenvalue as a function of mesh length and gradient inertia parameter is contained in Tables I and II for the membrane and bending problems, respectively. A one-hundred element, uniform grid is used with free-free boundary conditions to approximate the maximum eigenvalue in an infinite mesh. The maximum eigenvalue is obtained by the power method. The nondiagonal mass matrix is used as a standard in each case.

A gradient inertia parameter α equal to 0.75 in the diagonal mass matrix is seen to provide essentially the same maximum eigenvalues as the nondiagonal mass matrix for the membrane problem.*

A gradient inertia parameter α equal to 0.45 is seen to provide essentially the same maximum eigenvalues as the nondiagonal mass matrix.* It seems reasonable to expect that further work with these ideas will lead to better criteria for choosing specific values of the gradient inertia parameter α. Certainly more important is how the entire frequency spectrum is affected by α, rather than just the maximum frequency.

To obtain a mass matrix suitable for the original shell element, these ideas are carried over just as they stand. The equivalent entries in the consistent mass matrix are computed and added to form the diagonal terms of a diagonal mass matrix. The same gradient inertia scaling is used; one value for membrane and another value for bending. No rotatory inertia is included. The selection of the scaling values comes from the frequency considerations just covered.

---

* Tables I and II have been corrected from the original. They do not now support these choices of the gradient inertia scaling parameters. However, all of the conclusions of the paper remain the same. Only the details of the calculations will change with new values of these parameters.

TABLE I

Membrane Eigenvalues

Maximum Eigenvalues of $M^{-1}K_m$ and $M_d^{-1}K_m$ as a Function of Element Length and Gradient Inertia Scaling

		Element Length, ℓ										
		0.25	0.50	0.75	1.00	1.25	1.50	2.00	3.00	4.00	5.00	6.00
$M^{-1}K_m$		504	168	56	42	27	18	10	5	2.6	1.7	1.2
$M_d^{-1}K_m$	$\alpha = 0.50$	2177	547	242	137	87	61	34	15	8.6	5.5	3.8
	$\alpha = 0.75$	1461	365	161	91	58	40	23	10	5.8	3.7	2.6
	$\alpha = 1.00$	1094	273	123	69	44	30	17	8	4.3	2.8	1.9

TABLE II

Bending Eigenvalues

Maximum Eigenvalues of $M^{-1}K_b$ and $M_d^{-1}K_b$ as a Function of Element Length and Gradient Inertia Scaling

		Element Length, ℓ										
		0.25	0.50	0.75	1.00	1.25	1.50	2.00	3.00	4.00	5.00	6.00
$M^{-1}K_b$		$.64\times10^6$	40,200	7,950	2510	1030	497	157	31	10	4.0	1.9
$M_d^{-1}K_b$	$\alpha = .25$	2.78×10^6	160,000	31,900	10,090	5130	1990	631	124	39	16.1	7.8
	$\alpha = .45$	1.44×10^6	89,760	17,700	5610	2300	1110	351	69	22	9.0	4.3
	$\alpha = 1.0$	0.65×10^6	40,400	7,990	2530	1030	499	158	31	10	4.0	1.9

The same procedure is used in Reference [11] to form a diagonal mass matrix from the non-diagonal mass matrix prescribed by the finite element method. However, rotatory inertia is retained in Reference [11] in contrast to the approach taken here. The details on the choice of the scaling parameters are omitted.

4. TIME INTEGRATION

Due to its computational speed and entirely satisfactory performance when operating with a time step below the critical one, a central difference time integration is used. Without reference to either the membrane or bending behavior, the equations of motion are separated into the two first order equations shown in Equation (21).

$$\dot{p} + c^2 M^{-1} K q = 0$$
$$\dot{q} - p = 0 \tag{21}$$

Here, p is a velocity vector. Using a time step of Δt and a subscript of n to denote a point in time, these equations are differenced to obtain the Equations (22)

$$p_{n+\frac{1}{2}} = p_{n-\frac{1}{2}} - \Delta t c^2 M^{-1} K q_n$$
$$q_{n+1} = q_n + \Delta t p_{n+\frac{1}{2}} \tag{22}$$

Thus, given the velocities p at $n-\frac{1}{2}$ and the displacement q at n, the new velocities at $n + \frac{1}{2}$ and the new displacements at n+1 are computed with one pass. In theory, this is entirely equivalent to using a second central difference expression for the accelerations $\ddot{q}$ in either Equations (9) or (16) and using the old displacements at n and n-1 to get the new displacements at n+1. In practice, however, (22) is more accurate due to the finite word lengths of computers, [25].

It is also much more informative to know a velocity and a displacement at a given point in time rather than two successive displacements, albeit only a short calculation to get the velocities.

This integration scheme is only conditionally stable. To examine stability, it is more convenient to use the all-displacement version as shown in Equation (23).

$$q_{n+1} - 2q_n + q_{n-1} + \Delta t^2 c^2 M^{-1} K q_n = 0 \tag{23}$$

A solution in the form of Equation (24) is sought.

$$q_n = v e^{\beta n \Delta t} \tag{24}$$

Here β is undetermined and v is an arbitrary displacement shape. Substituting Equation (24) into Equation (23) provides the results in Equation (25).

$$(e^{\beta \Delta t} - 2 + e^{-\beta \Delta t} + \Delta t^2 c^2 M^{-1} K) v = 0 \tag{25}$$

This is an eigenvalue problem and for each eigenvalue there is a separate β. Denoting any given eigenvalue of $M^{-1}K$ by λ, the appropriate polynomial for β is given in Equation (26).

$$e^{\beta \Delta t} - 2 + e^{-\beta \Delta t} + \Delta t^2 c^2 \lambda = 0 \tag{26}$$

Since the motion in Equation (21) is bounded for all time, $|e^{\beta \Delta t}|$ must be less than 1. This leads to the requirement that $\Delta t^2 c^2 \lambda$ must be less than or equal to 4.

Since the maximum eigenvalue of $M^{-1}K$ provides the strictest condition, the limits on Δt become those in Equation (27).

$$\Delta t^2 \leq \frac{4}{c^2 \lambda_{max}} \tag{27}$$

Previous work in this area[26] shows that for the membrane problem, λ is proportional to $1/\ell^2$, the mesh length in a uniform mesh, and for the bending problem λ is proportional to $1/\ell^4$. Thus, empirical constants related to the differencing scheme or displacement assumptions and independent of element length and the constant c will give the expressions in Equation (28).

$$\Delta t \leq a_1 \frac{\ell}{c_m} \tag{28}$$

$$\Delta t \leq a_2 \frac{\ell^2}{c_b}$$

The first inequality is for the membrane problem, the second is the bending problem. If a combined membrane and bending response calculation is being made, then the strictest constraint will limit Δt. Table I shows that λ_{max} does vary as $1/\ell^2$ and a value of a_1 equal to 0.209 results for the membrane problem. In Table II, λ_{max} varies as $1/\ell^4$ and a value of a_2 equal to 0.0267 results for the bending problem.

The choices in the gradient inertia parameters based on a matching of the maximum eigenvalues give the nondiagonal and diagonal mass matrix the same stability constraints on time step size for this integration method. To apply these results to the general shell element, several adaptations must be made. For layered shells, an area density rather than space density is more appropriate. Equation (29) defines the area density r.

$$r(\theta,s) \equiv \int_{h^-}^{h^+} \rho(\theta,s,\zeta)d\zeta \tag{29}$$

The larger of the meridional or circumferential membrane moduli in the shell theory is used in place of the modulus E. Equation (30) defines this elastic constant.

$$C(\theta,s) \equiv \max\left(\int_{h^-}^{h^+} \frac{E_{\theta\theta}}{1-\nu_{s\theta}\nu_{\theta s}}\,d\zeta\ ,\ \int_{h^-}^{h^+} \frac{E_{ss}}{1-\nu_{s\theta}\nu_{\theta s}}\,d\zeta\right) \tag{30}$$

The larger of the meridional or circumferential bending moduli in the shell theory is used in place of $\frac{Eh^2}{12}$. Equation (31) defines this elastic constant

$$D(\theta,s) \equiv \max\left(\int_{h^-}^{h^+} \frac{\zeta^2 E_{\theta\theta}}{1-\nu_{s\theta}\nu_{\theta s}}\,d\zeta\ ,\ \int_{h^-}^{h^+} \frac{\zeta^2 E_{ss}}{1-\nu_{s\theta}\nu_{\theta s}}\,d\zeta\right) \tag{31}$$

Since meshing in general is irregular, in each element the minimum of the side lengths and diagonals is used in place of ℓ. Equation (32) defines this minimum distance δ.

$$\delta \equiv \min\ (\overline{ij}, \overline{jk}, \overline{k\ell}, \overline{\ell i}, \overline{ik}, \overline{j\ell}) \tag{32}$$

Thus, in each element a critical time step is computed, one based on membrane response and the other on bending response. The minimum obtained for the entire mesh must govern the integration. Equation (32) restates the time step constraints for the general shell element.

$$\Delta t \leq \min \left(0.209 \frac{\delta}{\sqrt{C/r}} \ , \ 0.0267 \frac{\delta^2}{\sqrt{D/r}} \right) \tag{32}$$

To account for boundary conditions, nonuniform meshing, nonhomogeneous materials, membrane and bending coupling and to improve accuracy, a value of Δt equal to 0.8 of critical is customarily used. For example, critical time step estimates have been worked out for the axial bending in cylindrical shells by Sobel[27], a case where the circumferential curvature makes the axial bending stiffer. It is reflected by a slight decrease in the critical time step for bending.

At a mesh length to thickness ratio of 2.25, both criteria give the same critical time step. The critical time step for smaller length to thickness ratios is controlled by the bending and for larger ratios by the membrane behavior.

5. NUMERICAL EXAMPLES

Three examples of the results of this work are enclosed. The first example is a very simple problem for which an exact solution is known. It is very difficult numerically since the solution is a propagating discontinuity. The second example is a bending problem where the stresses generated at a clamped boundary are examined. The last example is a cone problem without an exact solution but for which numerous other computations are available with which to make a comparison.

By putting a unit step in pressure on the end of a cylindrical shell of very large radius to thickness ration and zero Poisson's ratio a unit step in stress should propagate down the cylinder just as in a half space. Figure 3 shows the numerical results of this calculation along with the exact solution, the propagating discontinuity in stress.

Figures (3a) and (3b) show the temporal behavior of the stress pulse as it passes a fixed point along the cylinder. Figures (3c) and (3d) show the shape of the pulse at a fixed point in time. The time step used was controlled by bending and is one half of the critical membrane time step of the lumped mass system. The lumped mass results are much to be preferred over those from the consistent mass calculations. The overshoots in stress are less for the lumped mass results. Even in this ideal circumstance, the consistent mass calculations required twice the time to compute than the lumped mass results required. The early arrival time of a significant amount

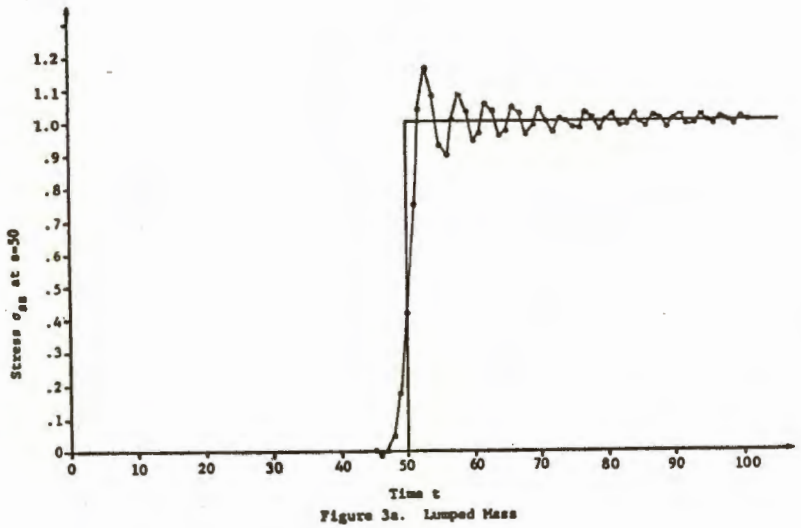

Figure 3a. Lumped Mass

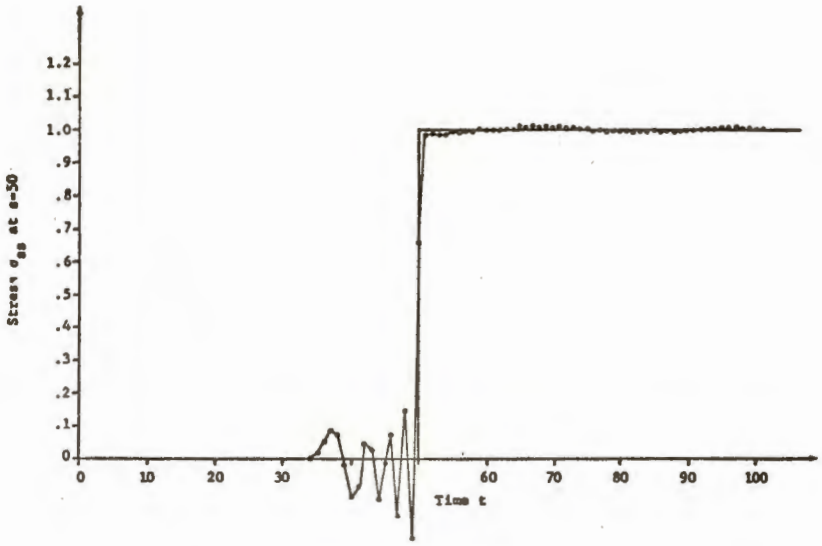

Figure 3b. Consistent Mass

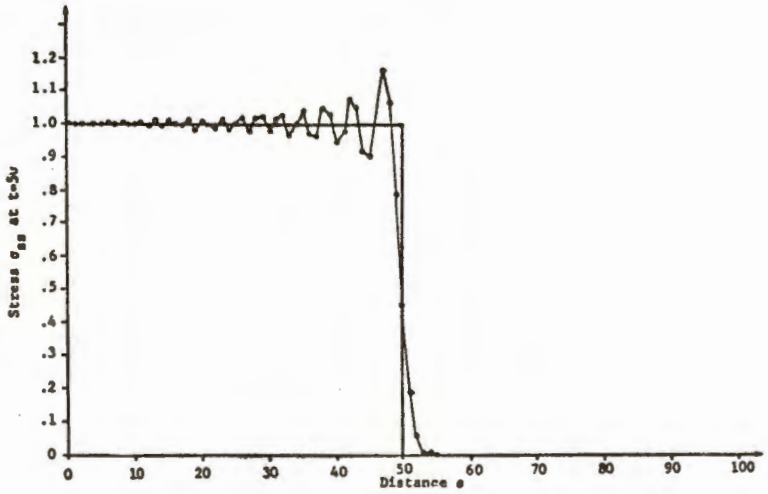

Figure 3c. Lumped Mass

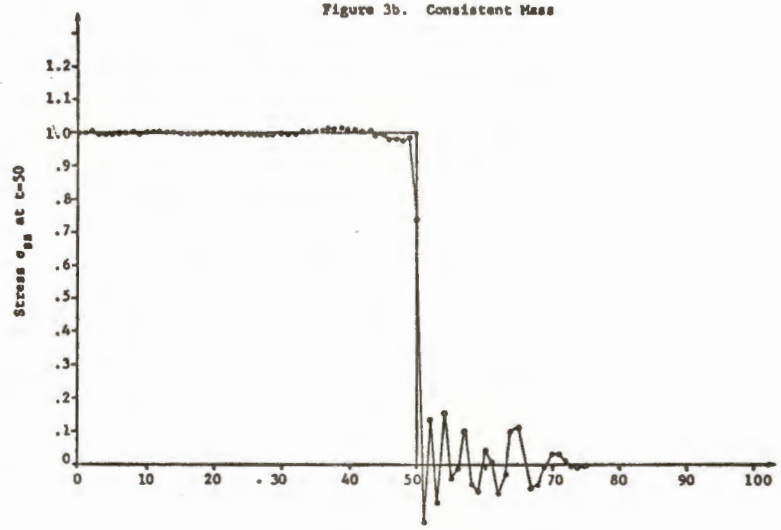

Figure 3d. Consistent Mass

Figure 3

The membrane response of a cylindrical shell struck on the end by a Heaviside pressure pulse. Modulus E=1, Poisson's ratio ν=0, density ρ=1, thickness h=1, radius r=10^{10}, length ℓ=100, mesh spacing Δs=1,time step Δt=1/11.

of information in the consistent mass calculations cannot be tolerated in more complicated problems. One of the most valuable checks of the correctness of an involved calculation is the arrival times of stress pulses at far boundaries and interfaces. It is frequently necessary to establish delay times between the point of impact and some other location on the structure and calculation where stresses arrive early cannot be reliably used.

The smearing of the discontinuity and oscillations are typical of virtually all of the common numerical integration schemes. The overshoot and oscillations in the numerical solutions just behind the discontinuity can be reduced, but only at the expense of further smearing of the front with artificial viscosity or implicit damping accompanying some integration schemes[9]. Shock matching or method of characteristics computer programs are able to improve on this solution. Both these techniques are used in one dimensional wave propagation calculations, but are inappropriate for the general shell problem of interest here.

A clamped cylindrical shell with a suddenly applied pressure responds early in time predominately in bending. Figure 4 shows the bending stresses at the clamped support and at two places removed from the support. A comparison is made with a bending solution developed by Forrestal, Sliter and Sagartz[27]. As can be seen, the agreement is quite good.

The last example is a problem from a series of check problems being assembled by the Lockheed Palo Alto Research Laboratories.

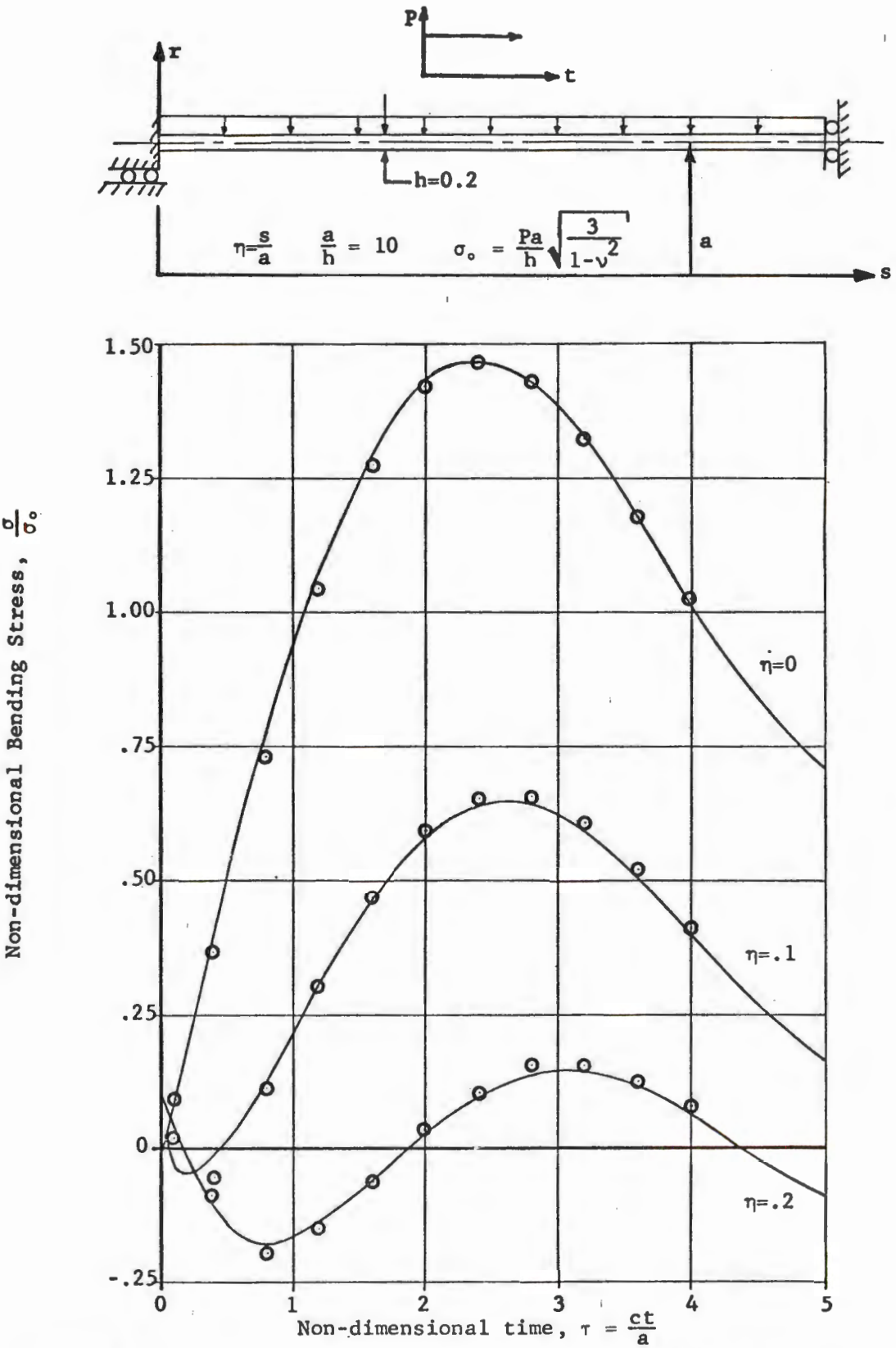

Figure 4. Bending response at a clamped support of a cylindrical shell.

It is a clamped-clamped conical frustum loaded with a half cosine initial radial velocity distribution. Figure 5 is a detailed statement of the problem. Figure 6 shows the mesh used and the point under the load for which the normal displacement is plotted. Figure 7 shows the normal deflection under the peak load as a function of time. The results from the present work and the other three computations are virtually identical. In view of the differences in these programs, both in space and time integrations, these results must be considered as correct and as a verification of all four efforts.

SLADE and the STAR program, a finite difference program at Lockheed, both use explicit time integration schemes, while DYNASØR and SABØR3/DRASTICII both use implicit time integration schemes. The critical time step for this problem is controlled by meridional bending at the small end of the cone. Expression (32) gives a critical time step of 1.03 μsec and a time step of 1 μsec was used in this analysis. A calculation made with a 1.06 μsec time step diverged.

While there does not presently exist enough information for timing comparisons with other schemes, it is clear that explicit methods are much faster per step than implicit methods. They are, however, constrained to function with very small time steps. It is interesting to note that whenever an explicit time integration method is used on a problem where high frequencies dominate, they are invariably

Material Properties

Homogeneous, isotropic, elastic

Young's Modulus = 3.52×10^6 psi

Poisson's Ratio = 0.286

Mass Density = 1.88×10^{-4} slugs/in^3

Boundary Conditions:

Clamped at Both Ends

Loading

Half Cosine Initial Velocity

Uniform along the Shell

V_o = 444. in/sec.

Meshing

18 x 15, Δt = 1 μsec

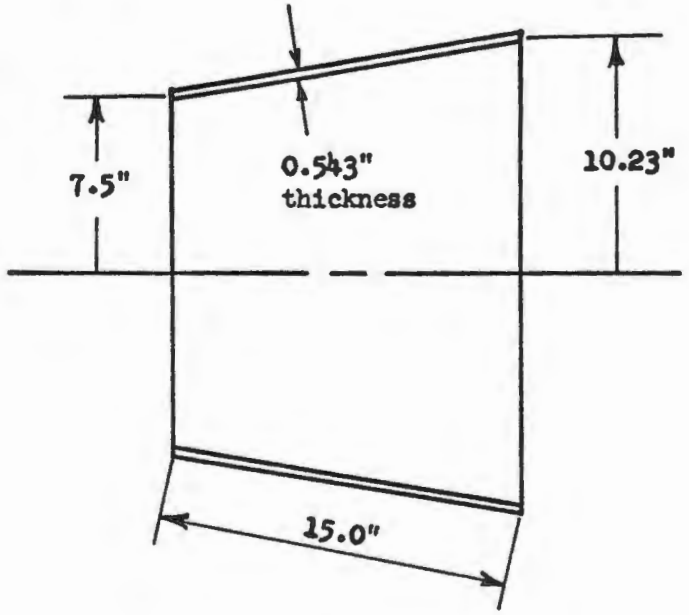

Figure 5 Dynamic Response of a Conical Shell

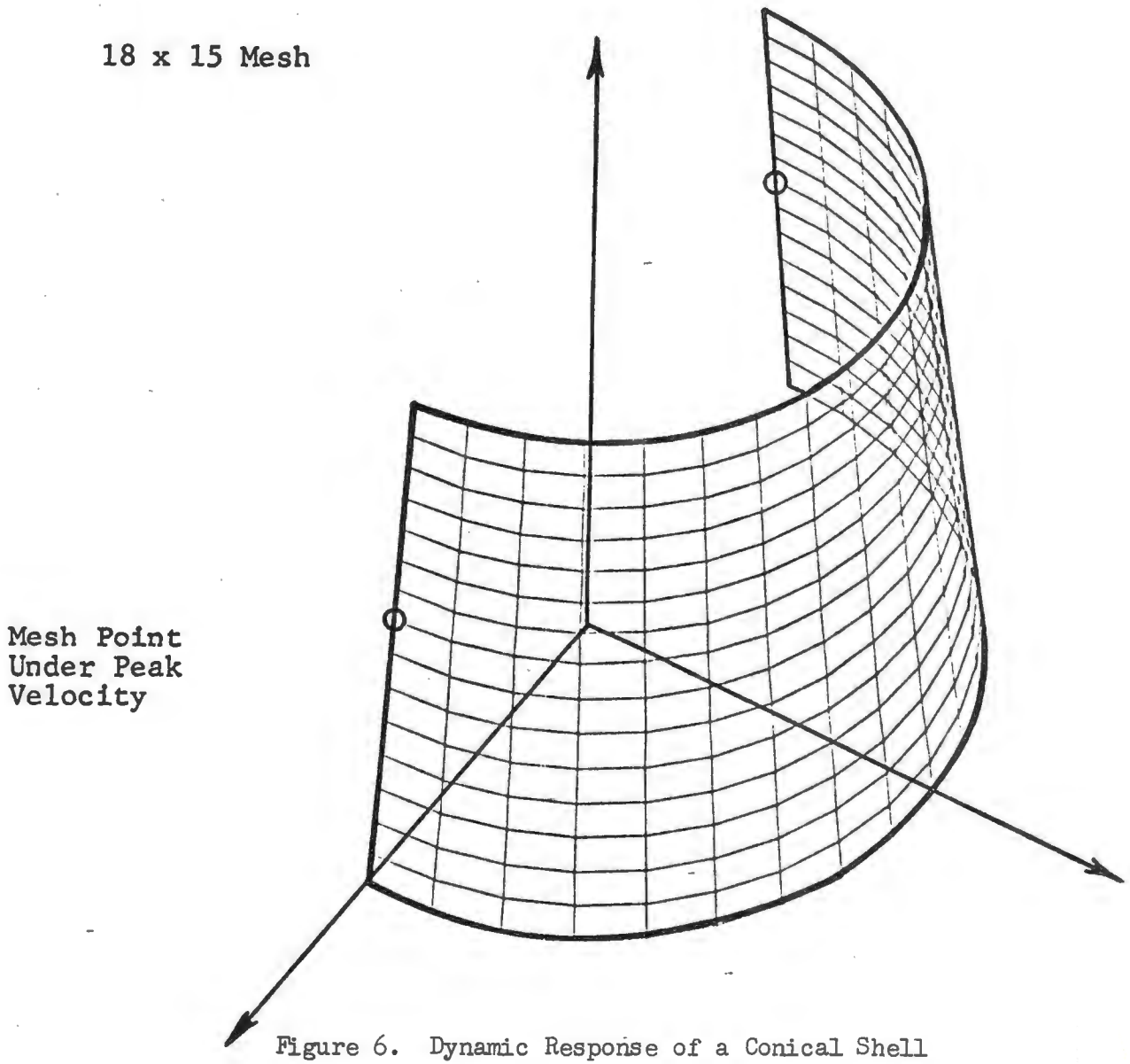

Figure 6. Dynamic Response of a Conical Shell

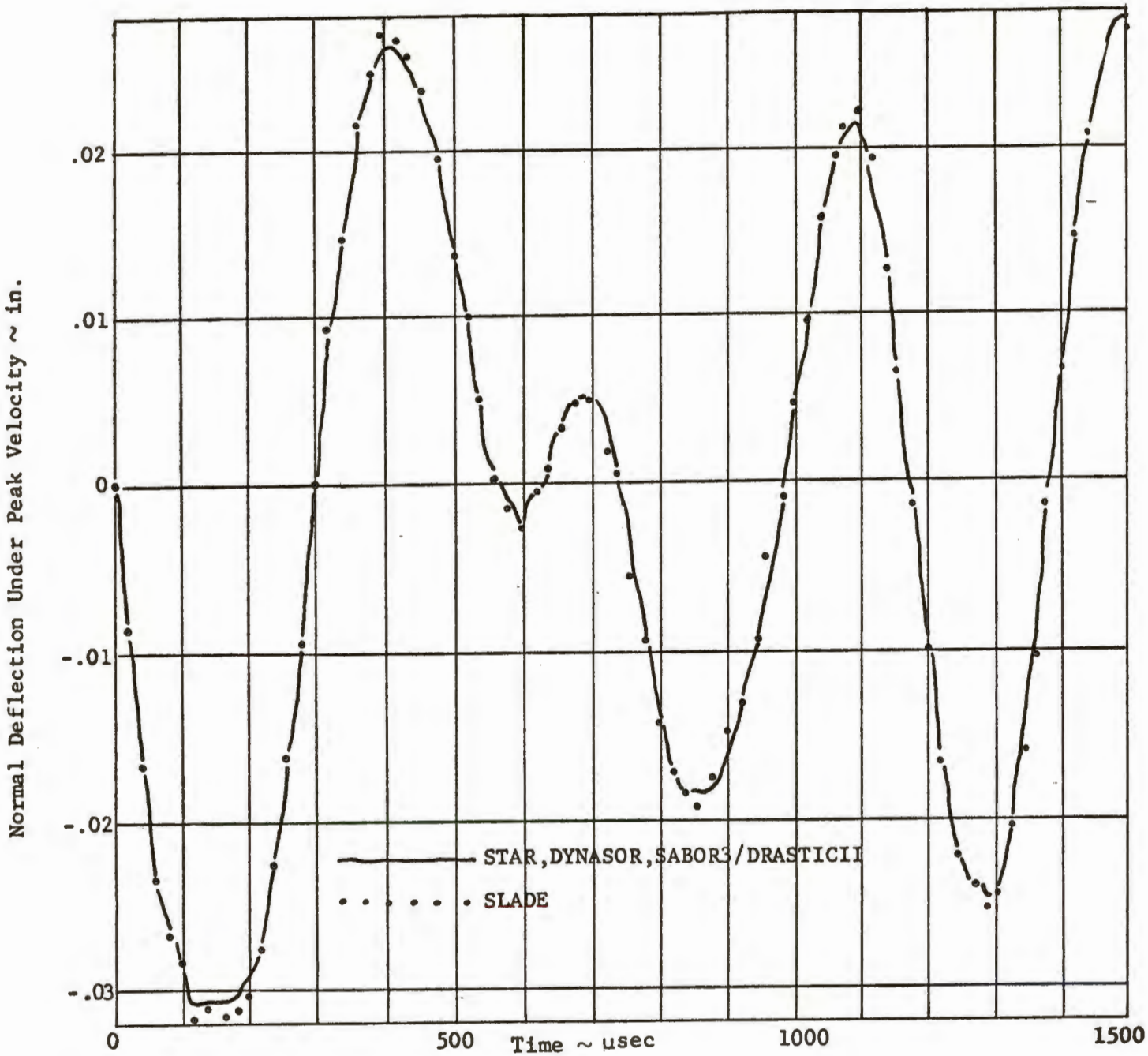
Normal Deflection Under Peak Velocity ~ in.
.02
.01
0
-.01
-.02
-.03
0
500
1000
1500
Time ~ μsec
STAR,DYNASOR,SABOR3/DRASTICII
SLADE

Figure 7

used with time steps that are equal to or less than the critical time step of the explicit central difference time integrator. In this case, accuracies are the same. For the present results on a CDC6600 computer, 1890 equations of motion are integrated per central processor second. With nine equations at each mesh point, that is equivalent to 210 mesh points per central processor second or 756,000 mesh points per central processor hour. The integration subroutine is largely the product of the stiffness matrix times the displacement vector. This subroutine has also been coded in the CDC machine language. When the calculations are carried out with this version of the subroutine, 5700 equations of motion are integrated per central processor second, or 630 mesh points per central processor second.

6. CONCLUSIONS

The present work has demonstrated a very viable transient dynamic response approach. It is based on the simplest of mass matrices and time integration schemes. The frequently heard complaint of instability is easily resolved by a study of stability and in practice the time step constraint is contained internally in the computer program and used to check the users requested time step and reduce it as necessary. It is a one-time operation that remains valid throughout the integration. The diagonal mass matrix is indistinguishable from its nondiagonal parent in the results and is much easier to handle from a computational and storage standpoint.

While this work was undertaken to provide a mass matrix for the shell element in SLADE, the approach is applicable to a wide class of shell elements. The bending behavior of virtually all shell elements when taken as flat and in one dimension is that of a beam element with cubic displacement assumptions and the membrane behavior will be that of a bar element with linear, quadratic or cubic displacement assumptions. Whenever this is the case, the present results apply.

Acknowledgement

For many helpful discussion, the authors are indebted to Raymond D. Krieg, Sandia Laboratories, whose knowledge and experience in these matters overshadows all others we have encountered. Special mention must also be made of Walter A. Von Riesemann, Sandia Laboratories, whose generosity with his extensive collection of finite element literature has proven extremely helpful.

REFERENCES

1. J. S. Archer, "Consistent Mass Matrix for Distributed Mass Systems," Journal of the Structural Division, Proceed. ASCE, August 1963.

2. J. S. Archer, "Consistent Matrix Formulations for Structural Analysis Using Finite-Element Techniques," AIAA Journal, Vol. 3, October 1965.

3. E. L. Wilson and R. W. Clough, "Dynamic Response by Step-by-Step Matrix Analysis," Symposium on the Use of Computers in Civil Engineering, Lisbon, Portugal, October 1962.

4. R. W. Clough and C. A. Felippa, "A Refined Quadrilateral Element for Analysis of Plate Bending," Proceedings of the 2nd Conference on Matrix Methods in Structural Engineering, Air Force Institute of Technology, Wright-Patterson Air Force Base, Ohio, October 1968.

5. R. W. Clough, "Analysis of Structural Vibrations and Dynamic Response," Japan-U. S. Seminar on Matrix Methods of Structural Analysis and Design, Tokyo, Japan, August 1969.

6. R. W. Clough and E. L. Wilson, "Dynamic Finite Element Analysis of Arbitrary Thin Shells," Conference on Computer Oriented Analysis of Shell Structures, Lockheed Palo Alto Research Laboratory, Palo Alto, California, August 1970.

7. S. Klein and R. J. Sylvester, "The Linear Elastic Dynamic Analysis of Shells of Revolution by the Matrix Displacement Method," Proceedings of the 2nd Conference on Matrix Methods in Structural Engineering, Air Force Institute of Technology, Wright-Patterson Air Force Base, Ohio, October 1968.

8. S. P. Chan, H. L. Cox and W. A. Benfield, "Transient Analysis of Forced Vibrations of Complex Structural-Mechanical Systems," Journal of the Royal Aeronautical Society, Vol. 66, July 1962.

9. J. A. Stricklin, J. E. Martinez, J. R. Tillerson, J. H. Hong and W. E. Haisler, "Nonlinear Dynamic Analysis of Shells of Revolution by Matrix Displacement Method," AIAA/ASME 11th Structures, Structural Dynamics, and Materials Conference, Denver, Colorado, April 1970.

10. J. C. Houbolt, "A Recurrence Matrix Solution for the Dynamic Response of Elastic Aircraft," Journal of the Aeronautical Sciences, Vol. 17, September 1950.

11. L. B. McWhorter, and W. E. Haisler, "FAMSOR-A Finite Element Program for the Frequencies and Mode Shapes of Shells of Revolution," SC-CR-715125, Sandia Laboratories Contractor Report, Albuquerque, New Mexico, October 1970.

12. C. C. Fu, "A Method for the Numerical Integration of the Equations of Motion Arising From a Finite Element Analysis," JAM, Vol. 37, September 1970.

13. R. de Vogelaere, "A Method for the Numerical Integration of Differential Equations of Second-Order Without Explicit First Derivatives," Journal of Research, National Bureau of Standards, Vol. 54, No. 3, 1955.

14. M. D. Olson and G. M. Lindberg, "Vibration Analysis of Cantilevered Curved Plates Using a New Cylindrical Shell Finite Element," Proceedings of the 2nd Conference on Matrix Methods in Structural Engineering, Air Force Institute of Technology, Wright-Patterson Air Force Base, Ohio, October 1968.

15. B. E. Greene, R. E. Jones, D. R. Strome and R. W. McLay, "Dynamic Analysis of Shells Using Doubly-Curved Finite Elements," Proceedings of the 2nd Conference on Matrix Methods in Structural Engineering, Air Force Institute of Technology, Wright-Patterson Air Force Base, Ohio, October 1968.

16. R. E. Nickell, "On the Stability of Approximation Operators in Problems of Structural Dynamics," International Journal of Solids and Structures, Vol. 7, pp. 301-319, 1971

17. G. L. Goudreau, "Evaluation of Discrete Methods for the Linear Dynamic Response of Elastic and Viscoelastic Solids," Report No. 69-15, Department of Civil Engineering, University of California, Berkeley, California, June 1970.

18. S. W. Key and R. D. Krieg, "Comparison of Finite Element and Finite Difference Methods," ONR Symposium on Numerical and Computer Methods in Structural Mechanics, Urbana, Illinois, September, 1971.

19. S. W. Key, "The Analysis of Thin Shells With a Doubly Curved Arbitrary Quadrilateral Finite Element," Conference on Computer Oriented Analysis of Shell Structures, Lockheed Palo Alto Research Laboratory, Palo Alto, California, August 1970.

20. S. W. Key and Z. E. Beisinger, "The Analysis of Thin Shells by the Finite Element Method," IUTAM Symposium on High Speed Computing of Elastic Structures, Liege, Belgium, August 1970.

21. S. W. Key and Z. E. Beisinger, "SLADE: A Computer Program for the Static Analysis of Thin Shells," SC-RR-69-369, Sandia Laboratories, Albuquerque, N. M., November 1970.

22. H. C. Martin, "Introduction to Matrix Methods of Structural Analysis," McGraw Hill Book Co., New York, 1966.

23. O. C. Zienkiewicz, "The Finite Element Method in Structural and Continuum Mechanics," McGraw Hill Book Co., New York, 1967.

24. J. S. Przemieniecki, "Theory of Matrix Structural Analysis," McGraw Hill Book Co., New York, 1968.

25. R. D. Krieg and H. C. Monteith, "A Large Deflection Transient Analysis of Arbitrary Shells Using Finite Differences," Conference on Computer Oriented Analysis of Shell Structures, Lockheed Palo Alto Research Laboratory, Palo Alto, California, August 1970.

26. R. D. Krieg and S. W. Key, "UNIVALVE, A Computer Code for Analyzing Large Deflection Elastic-Plastic Response of Beams and Rings," SC-RR-66-2692, Sandia Laboratories, Albuquerque, New Mexico, January 1968.

27. L. H. Sobel, "Analytical Study of Asymmetric Wave Propagation in Shells," Progress Report No. 13, NASA Contract NAS1-9111, Lockheed Palo Alto Research Laboratory, Palo Alto, California, June 1970.

28. M. J. Forrestal, G. E. Sliter, and M. J. Sagartz, "Stresses Emanating from the Supports of a Cylindrical Shell Produced by a Lateral Pressure Pulse," JAM, to appear.